Optical Characterization of Ultrananocrystalline Diamond Films

Daniel Franta [a,*] Lenka Zajíčková [a] Monika Karásková [a] Ondřej Jašek [a] David Nečas [a]
Petr Klapetek [b] Miroslav Valtr [b]

[a] *Department of Physical Electronics, Faculty of Science, Masaryk University, Kotlářská 2, 611 37 Brno, Czech Republic*
[b] *Czech Metrological Institute, Okružní 31, 638 00 Brno, Czech Republic*

Abstract

Optical properties of the ultrananocrystalline diamond films were studied by multisample method based on the combination of variable angle spectroscopic ellipsometry and spectroscopic reflectometry applied in the range 0.6–6.5 eV. The films were deposited by PECVD in a conventional bell jar (ASTeX type) reactor using dual frequency discharge, microwave cavity plasma and radio frequency plasma inducing dc self-bias at a substrate holder. The optical model of the samples included a surface roughness described by the Rayleigh-Rice theory and a refractive index profile in which Drude approximation was used. The results conformed with the present understanding of the polycrystalline diamond growth on the silicon substrate because the existence of silicon carbide and amorphous hydrogenated carbon film between the silicon substrate and nucleation layer was proved.

Key words: nanocrystalline carbon, optical properties characterization, band structure
PACS: 78.67.Bf, 95.75.Fg, 95.75.Hi

1. Introduction

Microcrystalline diamond finds several applications due to its high hardness but also as electronic and optical devices [1]. However, its roughness makes some applications difficult. A major advance was achieved in early 90ties when the crystalline size was decreased from down to nanometers [2]. However, the processes leading to the deposition of small grain-sized diamond films are not yet properly understood and these films exhibit different properties and morphology depending on the method of preparation. Therefore, the term "nanocrystalline diamond" (NCD) covers different materials such as columnary grown films with the grain sizes usually quoted below 100 nm (but 30 nm are nowadays possible) [3] and continuous dense coatings with grain sizes reaching 5–15 nm grown under high re-nucleation rates. The latter were firstly prepared by the group of D. M. Gruen [4] and the term ultrananocrystalline diamond (UNCD) was used in order to distinguish them from other films with the grain sizes below 100 nm.

In our previous paper the deposition of the UNCD films (crystal size below 10 nm) exhibiting very low roughness as compared to polycrystalline diamonds (rms of heights 9 nm), high hardness of 70 GPa and elastic modulus of 375 GPa was re-

* Corresponding author. Tel. +420-54949 3836; fax. +420-541211214.
Email address: `franta@physics.muni.cz` (Daniel Franta).

ported [5]. In this paper, the nucleation and beginning of the deposition of similar films are studied by optical measurements evaluated by our software procedures respecting surface roughness, refractive index profile and dispersion relations based on the parameterization of joint density of states (JDOS). Such approach allows to obtain information not only about the film optical constants but also about the nucleation and deposition process and material structure.

2. Experimental

The UNCD films were deposited on mirror polished silicon substrates by PECVD in a conventional bell jar (ASTeX type) reactor using dual frequency discharge, microwave (mw) cavity plasma (2.45 GHz) and radio frequency (rf) plasma (13.56 MHz) capacitively coupled to a substrate holder. The deposition mixture consisted of 9 % of CH_4 in H_2. The pressure and substrate temperature were 7.5 kPa and 1090 K, respectively. The plasma and radical densities were primarily determined by the mw discharge with the power of 850 W whereas the rf discharge (35 W), inducing a negative dc self-bias of -130 V, was used to control ion bombardment on the substrate. This method is a modification of bias enhanced nucleation (BEN) in which usually a dc bias is applied on the substrate [6]. The rf discharge was not switched off when finishing the nucleation phase but was kept during the whole deposition process in order to achieve a high re-nucleation rate necessary for the growth of UNCD films. The three samples were prepared changing the total preparation time from 5.5 to 7.5 min.

The optical characterization of the samples was based on variable angle spectroscopic ellipsometry and near-normal spectroscopic reflectometry. The Jobin Yvon UVISEL ellipsometer was employed for measurement of associated ellipsometric parameters representing three coordinates on Poincaré sphere defined as $I_{\mathrm{s}} = \sin 2\Psi \sin\Delta$, $I_{\mathrm{c,II}} = \sin 2\Psi \cos\Delta$ and $I_{\mathrm{c,III}} = \cos 2\Psi$. The measurements were carried out at five angles of incidence from 55° to 75° within the spectral range 0.6–6.5 eV. Reflectances R at angle of incidence of 6° were measured within the spectral range 1.2–6.5 eV using a spectrophotometer PerkinElmer Lambda 45. The morphology of sample surfaces was studied with the ThermoMicroscopes Explorer atomic force microscope (AFM).

3. Results and Discussion

It came out from modeling of optical data by various multilayer models that a good agreement between the measured and calculated data required at least three-phase model. This finding corresponds very well with commonly understood models of polycrystalline diamond (PCD) nucleation on silicon [1, 6]. A PCD is represented by the first phase. The second phase is associated with a prenucleation layer (PNL) and, obviously, the third phase is the Si substrate. This model is sufficient for relatively thick PCD films, i. e. , films being much thicker than the PNL.

In order to investigate sensitively the interface between our UNCD films and silicon the three samples with different thicknesses were prepared. Treating the measured optical data by a multisample method, a good agreement could be achieved only when taking into account inhomogeneous transition layers between the substrate and PNL as well as between the PNL and UNCD. The comparison of measured data and the best fit is given in Fig. 1.

The dielectric function profile of the transition layer between the substrate and PNL (TL1) could be modelled as a linear transition between c-Si and PNL materials. However, the profile of the transition layer between the PNL and UNCD turned to be more complicated. It was necessary to add a fourth phase, here called a nucleation phase (NP), which optical parameters were independent on the other three phases considered. Therefore, the transition layer between the PNL and UNCD was, in fact, represented by two transition layers TL2 and TL3, i. e. , a linear transition between the PNL and NP materials and between the NP and UNCD materials, respectively. The schematic representation of the whole structural model, that simultaneously

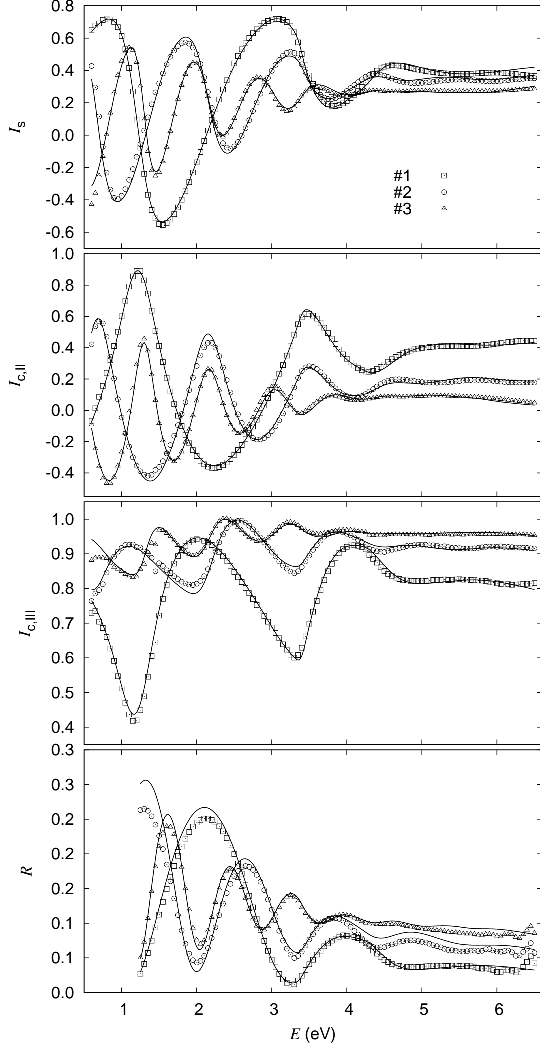

Figure 1. Spectral dependences of the associated ellipsometric parameters $I_{\rm s}$, $I_{\rm c,II}$, $I_{\rm c,III}$ and reflectance R for all three samples studied. The lines and symbols denote theoretical and experimental data, respectively. The ellipsometric data correspond to the angle of incidence of 65°.

shows the real profile of the optical constants obtained at 4.124 eV, is shown in Fig. 2. The total thicknesses d_1, d_2 and d_3 of the three samples under consideration are depicted by arrows in this profile too. There was a 121 nm homogeneous UNCD film in case of the thickest sample (#3) whereas the deposition process has been stopped already during the growth of inhomogeneous transition layer TL3 in case of samples #1 and #2.

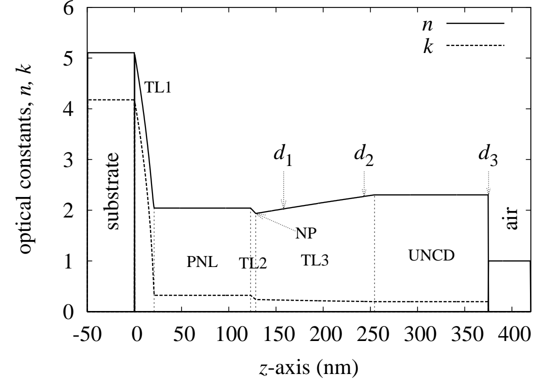

Figure 2. The structural model of the samples under study that shows the real profile of the optical constants n and k obtained at 4.125 eV. The total thicknesses d_1, d_2 and d_3 of the samples are depicted by arrows. For a detailed explanation of the particular layers see the text.

For an evaluation of the optical measurements the whole sample structure was described by a two-dimensional overall transfer matrix $\mathbf{M}$ because 2×2 matrix formalism [7] is very well suited for the description of multilayer and inhomogeneous structures. This formalism also offers an easy way for the description of a surface roughness that has to be taken into account in case of polycrystalline films too. Therefore, a final form of the matrix $\mathbf{M}$ for the sample #3 was

$$\begin{aligned}\mathbf{M} = {} & \mathbf{B}_{\rm RB}(\hat{n}_{\rm a}, \hat{n}_{\rm f}, \sigma, \tau)\times \\ & \mathbf{T}_{\rm UNCD}(\hat{n}_{\rm f}, t_{\rm f}, d - t_3 - t_2 - t_{\rm p} - t_1)\times \\ & \mathbf{T}_{\rm TL3}(\hat{n}_{\rm f}, \hat{n}_{\rm n}, t_3)\mathbf{T}_{\rm TL2}(\hat{n}_{\rm n}, \hat{n}_{\rm p}, t_2)\times \\ & \mathbf{T}_{\rm PNL}(\hat{n}_{\rm p}, t_{\rm p})\mathbf{T}_{\rm TL1}(\hat{n}_{\rm p}, \hat{n}_{\rm s}, t_1),\end{aligned} \tag{1}$$

where $\mathbf{B}_{\rm RB}$ is the boundary matrix representing rough surface, $\mathbf{T}_{\rm UNCD}$ and $\mathbf{T}_{\rm PNL}$ are the transfer matrices representing the homogeneous UNCD film and pre-nucleation layer, respectively, and $\mathbf{T}_{\rm TL1}$, $\mathbf{T}_{\rm TL2}$ and $\mathbf{T}_{\rm TL3}$ are the transfer matrices representing the inhomogeneous transition layers. All matrices are functions of system parameters and optical constants of i-th material n_i and k_i. The system parameters are rms of heights σ, autocorrelation length τ, total thickness of the multilayer structure d and thicknesses of particular lay-

ers TL3, TL2, PNL, TL1, i. e. t_3, t_2, t_p and t_1, respectively. The optical constants, i. e. complex refractive indices $\hat{n}_i = n_i - \mathrm{i}k_i$ are these of air $\hat{n}_\mathrm{a} = 1$, the UNCD film $\hat{n}_\mathrm{f}$, the nucleation phase $\hat{n}_\mathrm{n}$, the pre-nucleation layer $\hat{n}_\mathrm{p}$ and the substrate $\hat{n}_\mathrm{s}$.

It obvious that for thinner films, i. e. samples #1 and #2, Eq. (1) has to be modified as follows

$$\begin{aligned}\mathbf{M} = \; & \mathbf{B}_\mathrm{RB}(\hat{n}_\mathrm{a}, \hat{n}_\mathrm{x}, \sigma, \tau) \times \\ & \mathbf{T}_\mathrm{TL3}(\hat{n}_\mathrm{x}, \hat{n}_\mathrm{n}, d - t_2 - t_\mathrm{n} - t_1) \times \\ & \mathbf{T}_\mathrm{TL2}(\hat{n}_\mathrm{n}, \hat{n}_\mathrm{p}, t_2) \mathbf{T}_\mathrm{PNL}(\hat{n}_\mathrm{p}, t_\mathrm{p}) \times \\ & \mathbf{T}_\mathrm{TL1}(\hat{n}_\mathrm{p}, \hat{n}_\mathrm{s}, t_1),\end{aligned} \tag{2}$$

where $\hat{n}_\mathrm{x}$ is the complex refractive index on the surface expressed as

$$\hat{n}_\mathrm{x} = \sqrt{\frac{d - t_2 - t_\mathrm{p} - t_1}{t_3}(\hat{n}_\mathrm{f}^2 - \hat{n}_\mathrm{n}^2) + \hat{n}_\mathrm{n}^2}. \tag{3}$$

The boundary matrix representing rough surface was calculated using the Rayleigh-Rice theory (RRT) [8–10]. The AFM data on all three samples, as evaluated by the Gwyddion program [11], revealed that the rms of heights and autocorrelation length were 13–18 nm and 60–78 nm, respectively. Although, the rms of heights are slightly above the limits of the RRT, only this theory can be used to describe the roughness with such autocorrelation lengths [10]. The RRT is based, contrary to the effective medium approximation (EMA), on the solution of the Maxwell equations and includes, therefore, an effect of light scattering. The fitting results were in a relatively good agreement with AFM because resulting rms and autocorrelation lengths were in the ranges 13–16 nm and 46–59 nm, respectively.

The transfer matrices representing the inhomogeneous layers were calculated using an algorithm dividing recursively the inhomogeneous layer into sufficient number of inhomogeneous sublayers which transfer matrices were calculated by the Drude approximation. The final number of the sublayers is given by the condition that their thickness must be much lower than wavelength. More details about the applied algorithm can be found in [12].

The optical constants n_s and k_s of the c-Si were fixed at known values. The optical constants of all other three phases introduced in the structural model above were obtained from the dispersion formulae based on the parameterization of JDOS (PJ-DOS) [13]. In the frame of this model the interband transitions are expressed by three fitting parameters: minimum energy of transition, i. e. band gap E_g, maximum energy of transition E_h and parameter Q proportional to the density of states. Phases of the structural model were modelled by two or three different kinds of interband transitions. The parameters obtained from the best fit are summarized in Table 1. The dispersion behaviors of the optical constants are compared in Fig. 3 with data tabulated for the crystalline diamond [14] and a typical hydrogenated DLC film studied before [13].

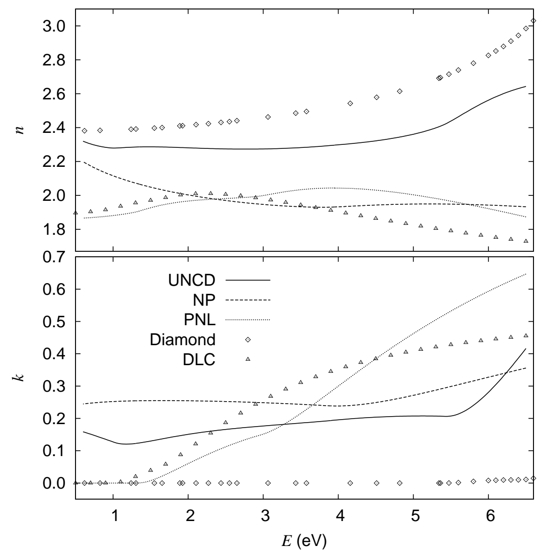

Figure 3. Spectral dependences of the refractive indices n and extinction coefficients k for UNCD film, nucleation phase (NP) and pre-nucleation layer (PNL). The optical constants of the crystalline diamond [14] and typical DLC film studied before [13] are added for a comparison.

From the resulting optical constants and parameters describing JDOS some information about particular material phases composing the prepared samples can be obtained. The first phase observed as a homogeneous UNCD top layer has the refractive index almost as high as diamond exhibiting also quite similar dispersion behavior (see Fig. 3).

Table 1
The parameters of the PJDOS dispersion models of the pre-nucleation layer (PNL), nucleation phase (NP) and ultrananocrystalline diamond (UNCD) film. For comparison, the parameters corresponding to a typical DLC studied before [13] are given in the last column.

parameters	PNL	NP	UNCD	DLC
Q_a [eV$^{3/2}$]	36.7	46.2	1.48	4.8
$E_{\mathrm{g}a}$ [eV]	1.33	0	0	1.0
$E_{\mathrm{h}a}$ [eV]	27.6	38.2	3.99	8.6
Q_b [eV$^{3/2}$]	64.6	282	80.7	180
$E_{\mathrm{g}b}$ [eV]	2.96	3.85	1.01	1.6
$E_{\mathrm{h}b}$ [eV]	29.4	89.8	48.4	70
Q_c [eV$^{3/2}$]	–	–	81.7	–
$E_{\mathrm{g}c}$ [eV]	–	–	5.42	–
$E_{\mathrm{h}c}$ [eV]	–	–	21.4	–

However, the extinction coefficient differs from zero in the whole spectral range 0.6–6.5 eV. This absorption can be divided into three regions (i) 5.4–6.5 eV, (ii) 1.0–5.4 eV and (iii) 0.6–1.0 eV. The absorption in deep UV is related to $\sigma \to \sigma^*$ interband transitions in diamond crystals. They correspond to c excitations included in the PJDOS dispersion model of the UNCD phase (see parameters Q_c, $E_{\mathrm{g}c}$ and $E_{\mathrm{h}c}$ in Table 1). It is important to note that obtained band gap $E_{\mathrm{g}c} = 5.42$ eV agrees very well with the indirect band gap of crystalline diamond, 5.48 eV [15]. However, the absorption is higher due to higher degree of disorder caused by a limited size of crystals in the UNCD material. The absorption in the middle spectral region can be assigned to $\pi \to \pi^*$ interband transitions in amorphous carbon phase at the boundaries between nanocrystals. When comparing the PJDOS parameters of the b excitations with the parameters of typical DLC included in Table 1 it is apparent that they describes both, the $\pi \to \pi^*$ and $\sigma \to \sigma^*$ interband transitions in amorphous carbon phase. The absorption in near IR can be associated with localized states close to the Fermi energy (a excitations with $E_{\mathrm{g}a} = 0$ eV) related to dangling bonds.

The optical constants of the PNL phase, observed as a homogeneous layer close to the substrate (see structural model in Fig. 2), resemble the optical constants of typical hydrogenated DLC studied before. However, the PJDOS parameters presented in Table 1 cannot be directly related to particular $\pi \to \pi^*$ and $\sigma \to \sigma^*$ excitations existing in DLC. It can be caused by the fact that the optical constants of this phase are not determined with high precision because the thicknesses of our samples were too high to measure the optical properties of the PNL directly without the additional phases. Anyway, the association of the PNL with hydrogenated DLC is in agreement with the nucleation mechanism presented by Kulisch [6].

Thin transition layer TL1 close to the c-Si substrate was modelled as a mixture transiting linearly from c-Si to DLC. Since a linear combination of dielelectric functions of c-Si and DLC approximates SiC, the TL1 corresponded to this material and it was not necessary to model this layer by an independent SiC phase of the structural model. The existence of SiC layer formed on the silicon substrate during the BEN of diamond has been already documented in the literature and its thickness of 21 nm, as found from the fit, agrees with the thickness estimated from the FTIR measurements to be about of 25 nm [6, 16].

4. Conclusion

The optical characterization of the UNCD films on the crystalline silicon turned to be a complex problem that included description of a surface roughness and refractive index profile. It is worth to notice that commercially available procedures could be hardly used for this purpose and, therefore, own software for simultaneous fitting of ellipsometric and reflectance measured data was used. The Rayleigh-Rice theory had to be used for the roughness description because the lateral dimensions of the roughness were comparable with the wavelength. Modeling of refractive index profile resulted in the multilayer four phase structure of the samples. The result conformed with the present understanding of the polycrystalline diamond growth on the silicon substrate because the existence of silicon carbide and amorphous hydrogenated carbon film between the silicon substrate and nucleation

layer was proved.

Acknowledgements

This work was supported by Ministry of Education of the Czech Republic (MSM0021622411), by Grant Agency of Czech Republic (202/05/0607) and by Czech Academy of Sciences (KAN311610701).

References

[1] J. Asmussen, D. K. Reinhard (Eds.), Diamond Films Handbook, Marcel Dekker, New York, 2002.

[2] T. P. Ong, W. A. Chiou, F. R. Chen, R. P. H. Chang, Carbon 28 (1990) 799.

[3] O. A. Williams, M. Daenen, J. D'Haen, K. Haenen, J. Maes, V. V. Moshchalkov, M. Nesládek, D. M. Gruen, Diamond Relat. Mater. 15 (2006) 654.

[4] D. M. Gruen, Annu. Rev. Mater. Sci. 29 (1999) 211.

[5] Z. Frgala, O. Jašek, M. Karásková, L. Zajíčková, V. Buršíková, D. Franta, J. Matějková, A. Rek, P. Klapetek, J. Buršík, Czech. J. Phys. 56 (2006) B1218.

[6] K. Kulisch, Deposition of Diamond-Like Superhard Materials, Springer-Verlag, Berlin, 1999.

[7] I. Ohlídal, D. Franta, Ellipsometry of thin film systems, in: E. Wolf (Ed.), Progress in Optics, Vol. 41, Elsevier, Amsterdam, 2000, pp. 181–282.

[8] S. O. Rice, Commun. Pure Appl. Math. 4 (1951) 351.

[9] D. Franta, I. Ohlídal, Opt. Commun. 248 (2005) 459.

[10] D. Franta, I. Ohlídal, J. Opt. A-Pure Appl. Opt. 8 (2006) 763.

[11] `http://gwyddion.net/`

[12] D. Franta, I. Ohlídal, 12th Slovak–Czech–Polish Optical Conference on Wave and Quantum Aspects of Contemporary Optics, Vol. 4356 of Proc. SPIE, 2001, pp. 207–212.

[13] D. Franta, V. Buršíková, D. Nečas, L. Zajíčková, Diamond Relat. Mater., submitted

[14] D. F. Edwards, H. R. Philipp, Cubic carbon (diamond), in: E. Palik (Ed.), Handbook of Optical Constants of Solids, Vol. I, Academic Press, New York, 1985, pp. 665–673.

[15] P. Y. Yu, M. Cardona, Fundamentals of Semiconductors, Springer, Berlin, 2001.

[16] W. Kulisch, L. Ackermann, B. Sobisch, Phys. Status Solidi A-Appl. Mat. 154 (1996) 155.